Available online at www.sciencedirect.com
ScienceDirect
Trans. Nonferrous Met. Soc. China 23(2013) 2957−2961
Transactions of Nonferrous Metals Society of China
www.tnmsc.cn

Improvement of adhesion properties of TiB_2 films on 316L stainless steel by Ti interlayer films

Mu-jian XIA, Hong-yan DING, Guang-hong ZHOU, Yue ZHANG

Jiangsu Provincial Key Laboratory for Interventional Medical Devices,
Huaiyin Institute of Technology, Huai'an 223001, China

Received 6 September 2012; accepted 17 May 2013

Abstract: The periodic $[Ti/TiB_2]_n$ (n=1, 2, 3) multilayered films were prepared on the substrate of AISI 316L stainless steel by magnetron sputtering to enhance the adhesion of TiB_2 films based on the remarkable mechanical performance of layered films. The influence of periods on microstructure, adhesion and hardness of $[Ti/TiB_2]_n$ multilayered films was studied. X-ray diffraction (XRD) analysis shows that the monolayer TiB_2 films exhibit (001) preferred orientation, and the preferred orientation of $[Ti/TiB_2]_n$ multilayered films transfers from (001) to (100) with the increase of periods. The cross-sectional morphology of each film displays homogeneity by field emission scanning electron microscopy (FESEM). The hardness of the films measured via nanoindention changes from 20 to 26 GPa with the increase of periods. These values of hardness are a bit lower than that of the monolayer TiB_2 films which is up to 33 GPa. However, the $[Ti/TiB_2]_n$ multilayered films present a considerably good adhesion, which reaches a maximum of 24 N, in comparison with the monolayer TiB_2 films according to the experimental results.
Key words: multilayered films; adhesion; TiB_2 films; magnetron sputtering; nano-hardness

1 Introduction

Titanium diboride (TiB_2), which is well known to be a ceramic compound, possesses numbers of excellent mechanical, physical, and chemical properties, such as high hardness, good wear and corrosion resistance, high electrical and thermal conductivity, and good chemical stability [1,2]. Such superior properties of TiB_2 make it to be investigated extensively for various applications of hard coatings, corrosion-resistance coatings, and diffusion barrier films used for microelectronic devices [3,4]. The monolayer TiB_2 films are deposited by various PVD methods, among which magnetron sputtering is considered an easier approach to prepare TiB_2 films owing to its relatively high deposition rate and low deposition temperature applied to the substrate [5,6]. However, it is difficult to produce the monolayer TiB_2 films with good mechanical integrities which are suitable for commercial and engineering applications [7]. The main problem is that the sputtered TiB_2 films are too brittle and have a poor adhesion due to the high residual stress [8]. The adhesion of TiB_2 coatings sputtered on high-speed steel is lower than 5 N [7,9]. The high residual stress generated in films can influence their properties directly, e.g. adhesion, fatigue strengthen, bond strength, tribological properties, etc [10−12]. Furthermore, excessive residual stress existed in the films may cause the formation of defects and delamination at the interface. In fact, compared with other mechanical properties, the adhesion directly affects operating life of the films, especially for which applied in tribological application.

Recently, many attempts have been made to enhance the adhesion of monolayer TiB_2 films. BERGER et al [12] found that the adhesion of TiB_2 coatings deposited by switching the substrate bias from negative to positive was significantly improved by nearly 60% in comparison with the films without applying bias. PANICH and SUN [13] reported that applying a bias on the TiB_2 coatings could enhance the adhesion. In addition, BOHWAN et al [14] also found that the nitride layer could greatly improve the adhesion of TiB_2 films sputtered on H13 steel.

The structure of nacre consisted of inorganic and organic constituents. Many researchers reported that the

Foundation item: Project (51175212) supported by the National Natural Science Foundation of China
Corresponding author: Hong-yan DING; Tel/Fax: +86-517-83559130; E-mail: xjmhyit@yahoo.com.cn
DOI: 10.1016/S1003-6326(13)62820-4

soft organic layer of nacre could erase the stress derived from the hard inorganic layer [15]. For example, the adhesions of TiN and AlN were greatly enhanced owing to the fabrication of Ti/TiN [16] and Al/AlN [17]. Consequently, in this work, the metallic titanium film was considered a soft layer, and was attempted to strengthen the adhesion of TiB_2 films based on this unique structure of nacre. Besides, the metallic titanium, which had a similar crystal structure with TiB_2, may decrease the mismatch between TiB_2 films and substrate, and combine with a hard layer TiB_2 to fabricate the bilayerd or multilayered films. The microstructure, hardness and adhesion of the monolayer TiB_2 films and $[Ti/TiB_2]_n$ multilayered films (n was the period of films) were investigated. Furthermore, the effects of periods on adhesion of multilayered films with various periods were discussed in details.

2 Experimental

A monolayer TiB_2 films and $[Ti/TiB_2]_n$ multilayered films were fabricated by magnetron sputtering. For the sputtering targets, a sintered TiB_2 target (99.9%) and a metallic Ti target (99.95%) of 50 mm in diameter were used. The Ti and TiB_2 targets were placed in the chamber at a substrate-magnetron distance of 50 mm. AISI 316L stainless steel (SS) was selected as the substrate specimens and cut to the dimensions of 10 mm×10 mm×1 mm. The specimens were grinded with 2000 grit water-proof silicon carbide papers, and then were treated by the electrochemical polishing. Subsequently, the specimens were ultrasonically cleaned in ultrasonic baths of acetone and ethanol. Finally, under the sputtering power of 60 W, the substrates were cleaned by Ar^+ (a high purity of 99.9%) etched at 4 Pa for 10 min prior to the deposition processes. The deposition chamber was evacuated to the pressure of 5×10^{-5} Pa before deposition. During deposition of all films, the Ar gas flow with 20 mL/min was introduced into the vacuum chamber. For the monolayer TiB_2 films, it was deposited by a r.f. power of 120 W, a working pressure of 0.7 Pa and a substrate temperature of 350 °C. For the $[Ti/TiB_2]_n$ multilayered films, Ti layer and TiB_2 layer were successively prepared on AISI 316LSS. A d.c. power of 40 W and a substrate temperature of 150 °C were applied to the deposition of Ti layer (25 nm). TiB_2 layer (125 nm) was prepared by the processing parameters of TiB_2 films. $[Ti/TiB_2]_n$ multilayered films were alternatively fabricated by the mechanical shutter, and were deposited with n=1, 2, 3.

The film structures were characterized by Thermo ARL X'TRA X-ray diffraction (XRD) equipped with Cu K_α radiation, and the measurement angle (2θ) was in the range from 20° to 80° with 0.02° interval. The cross-sectional morphology of films was observed by Hitachi Limited S4800II field emission scanning electron microscopy (FESEM). Hysitron Triblab nanoindentation with a Berkovich indenter was employed to determine the hardness of films using load—displacement curve. The principle of nanoindentation was specifically introduced in Ref. [18]. For the purpose of statistics and reliability, three indentations were made in each experiment to find the average hardness results. Since a critical load for the onset of a film failure was generally accepted as a relatively accurate measurement to estimate the adhesion, scratch test was recommended to investigate the adhesion. The adhesion was evaluated from the point where an acoustic emission profile and corresponding friction coefficient had an abrupt change during a scratch test.

3 Results and discussion

3.1 Crystalline structures

The XRD patterns of a monolayer TiB_2 films and $[Ti/TiB_2]_n$ multilayered films with various periods deposited on AISI 316LSS substrate are shown in Fig. 1. The peaks of AISI 316LSS (γ-Fe phases) were obvious. The monolayer TiB_2 films had the diffraction peaks of (001) and (100), but the intensity of (001) peak was higher than that of (100) peak. This indicates that the microstructure of TiB_2 films exhibited a preferred (001) orientation of TiB_2 crystalline. This preferred orientation was also formed when sputtered on Si (100) substrate [19]. The phenomenon can be interpreted that the films on substrates generally grow with the plane of the lowest surface free energy parallel to the film surface.

From Fig. 1, it can be also found that the $[Ti/TiB_2]_n$ multilayered films with various periods clearly exhibited diffraction peaks, and the mutual relation of magnitude changed with the increase of periods. For Ti layers, the intensity of (100) peaks gradually strengthened with the

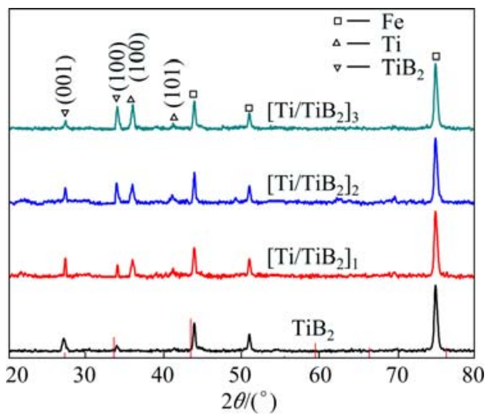

Fig. 1 XRD patterns of monolayer TiB_2 film and $[Ti/TiB_2]_n$ multilayered films deposited on AISI 316LSS with various periods

increase of periods. Whereas, the intensity of (101) peaks weakened and appeared to be opposite with that of (100) peaks. For TiB_2 layers, the intensity of (100) peak started to strengthen with the increase of periods, and it had a higher intensity than (001) peaks. This may be caused by the change in a degree of the preferred Ti (100) orientation which favored the epitaxial growth of TiB_2 (100) peaks. All the above results suggested that $[Ti/TiB_2]_n$ multilayered films with 3 periods exhibited preferred Ti (100) and TiB_2 (100) orientation. The preferred orientation was also found in the sputtered Ti/TiN multilayered films [20].

3.2 Cross-sectional morphology

Figure 2 presents the cross-sectional images of the monolayer TiB_2 films and $[Ti/TiB_2]_n$ multilayered films. From Fig. 2, it can seen that the $[Ti/TiB_2]_n$ multilayered films were composed of Ti layers (25 nm) and TiB_2 layers (125 nm) which were deposited alternatively. FESEM analysis of all the films displayed a very good morphology, and the cross-section possessed extremely dense and homogeneous.

3.3 Hardness

Figure 3(a) presents the load—penetration depth curves from nanoindentation measurement of $[Ti/TiB_2]_n$ multilayered films together with the monolayer TiB_2 films. The hardness values were calculated according to the corresponding load—penetration data, as shown in Fig. 3(b). It was observed that the hardness of multilayered films strongly depended on the periods. In the case of $[Ti/TiB_2]_1$, a relatively low hardness of 20 GPa was obtained. With the increase of periods, the hardness enhanced to a maximum value of 26 GPa that was found in $[Ti/TiB_2]_3$ multilayered films. It was similar to the hardness of TiB_2 films sputtered on nitrided AISI H13 steel ranging from 20 to 30 GPa [14]. The hardness of multilayered films was enhanced with the increase of periods due to the more interfaces generated between Ti and TiB_2 layers. As we all know that there were many imperfections at the interfaces between Ti and TiB_2 because of the crystal lattice mismatch. Meanwhile, the $[Ti/TiB_2]_n$ multilayered films with more periods had more interfaces, and the dislocation motioned more difficulty [21]. Furthermore, the grain size decreased in TiB_2 films with the increase of period enhanced the hardness of the multilayered films [22].

However, compared with the hardness of the monolayer TiB_2 films up to 33 GPa, the weakness of multilayered films hardness could be attributed to the effect of adjacent Ti soft layer. As a result of the diffusion of atoms between Ti layer and the adjacent TiB_2 layer, the interfaces of multilayered films turned to be compositionally gradient zone, which leaded to the lost of hardness enhancement. On the contrary, the significant hardness enhancement was observed in the Ti/TiB_2 multilayered films with the modulation period ranging from 1.1 to 9.8 nm in comparison with the Ti and TiB_2 monolayer films [23]. As known to all, the multilayered films with small modulation period had less time for ion bombardment at each target, which resulted in the incomplete growth process. Then the sharp interfaces were generated in films. Therefore, the crack propagation was reduced, and the hardness of multilayer

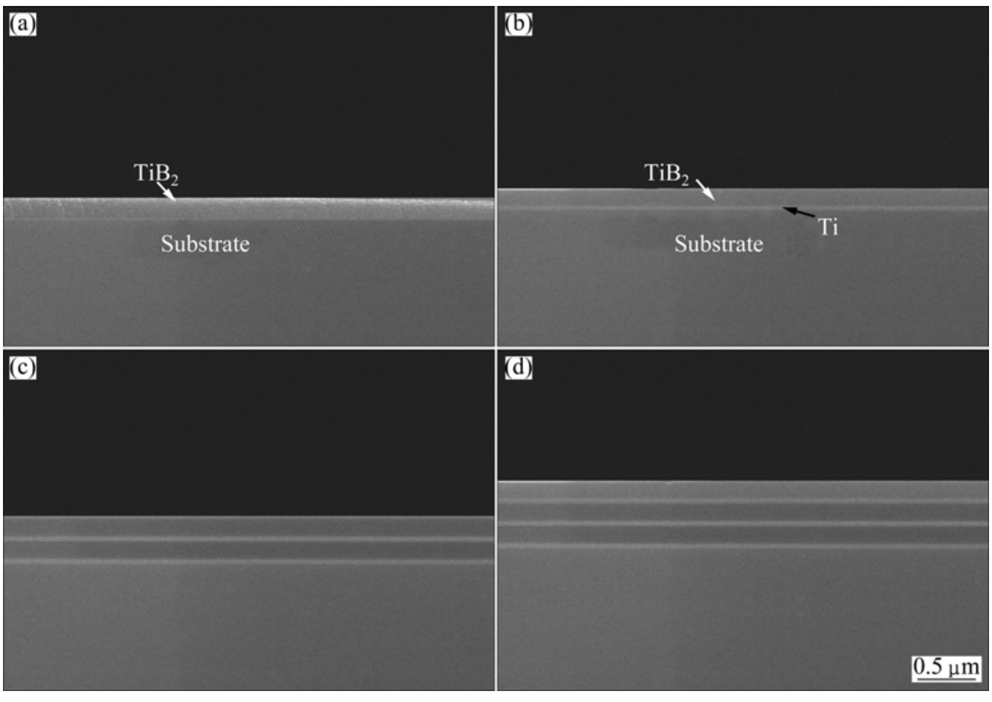

Fig. 2 Cross-sectional morphologies of a monolayer TiB_2 film (a), multilayered films $[Ti/TiB_2]_1$ (b), $[Ti/TiB_2]_2$ (c) and $[Ti/TiB_2]_3$ (d)

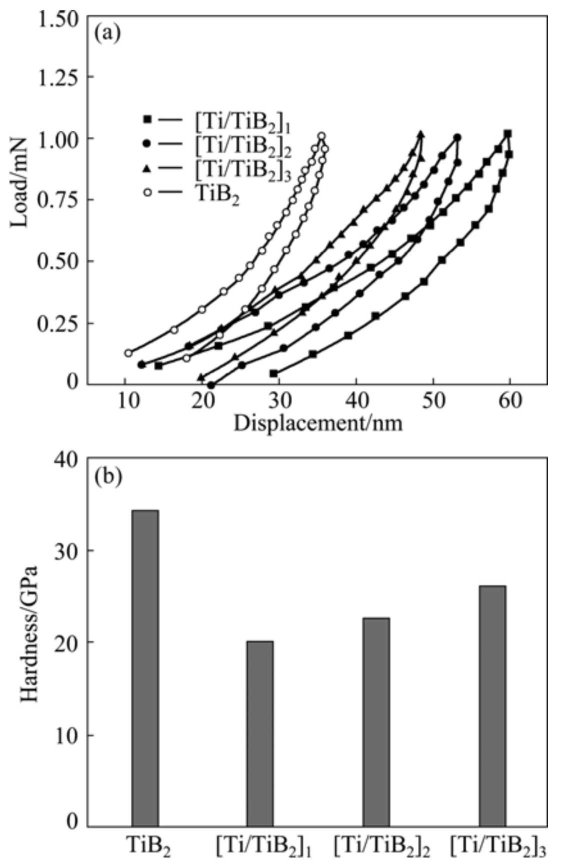

Fig. 3 Load—penetration depth curves (a) and hardness (b) of monolayer TiB_2 film and $[Ti/TiB_2]_n$ multilayered films with n=1, 2, 3

films with small modulation period was enhanced.

3.4 Adhesion

Variations of the critical load obtained from scratch test of the monolayer TiB_2 films and $[Ti/TiB_2]_n$ multilayered films are shown in Fig. 4. It was clearly found that the critical load of all multilayered films is higher than that of the monolayer TiB_2 films with the adhesion of 9.5 N. This phenomenon was also found by HAN et al [24] in Ti/TiN films. One possible reason was that the soft Ti layer could prevent the propagation of cracks generated in a brittle TiB_2 layer into a deeper layer. On the other hand, the enhancement of adhesion may be the result of the change of residual stress caused by ion bombardment during deposition. It was well accepted that the residual stress of films sputtered on diverse substrates presented difference, and the films sputtered with a higher stress also showed a poor adhesion strength. Consequently, the stress state of the monolayer TiB_2 films directly deposited on AISI 316LSS must be different from that prepared on Ti films. The interfaces of multilayered films were favorable to decrease the compressive stress, and the $[Ti/TiB_2]_n$ films with compressive stress states of alternating component layers processed a relative lower compressive stress compared with the monolayer TiB_2 films. This tendency was also found in Al/AlN multilayered films [17].

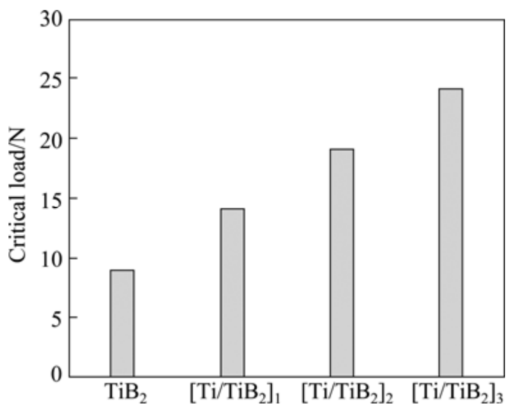

Fig. 4 Critical load of monolayer TiB_2 film and $[Ti/TiB_2]_n$ multilayered films with n=1, 2, 3

Additionally, it was clearly found that the critical load of multilayered films enhanced with the increase of periods. This enhancement may be related to the stress and periods of multilayered films. The more the periods were, the more the interfaces were between Ti and TiB_2, which can generally change the direction of the initial crack when it penetrated deep into the films [25]. The dislocations propagation of multilayered films which had more interfaces was easy to be inhibited. It also resulted in the failure of multilayered films during the scratch process [26,27].

On the other hand, the interface between a soft Ti layer and a brittle TiB_2 layer can store a part of total elastic energy during scratch loading, and the corresponding elastic energy at the interface between multilayered films and substrate was reduced [28]. With the increase of periods, the multilayered films presented more interfaces which can store more elastic energy and decline the stress effectively.

4 Conclusions

1) XRD patterns shows that the monolayer TiB_2 films exhibits the preferred orientation of (001), and the multilayered films with 3 periods presents the preferred orientation of TiB_2 (100) and Ti (100).

2) The cross-sectional morphology of each film processes homogeneous.

3) The interpretation for this hardness enhancement in $[Ti/TiB_2]_n$ multilayered films are based on interfaces acting on dislocations, which will contribute to the increase of hardness of the multilayer films. The hardness of multilayered films varies from 20 to 26 GPa with the increase of periods, but it has a little lost compared with the monolayer TiB_2 films (up to 33 GPa).

4) Such multilayer films with more periods will be quite favorable for commercial application in the future. A good adhesion of the $[Ti/TiB_2]_3$ multilayered films is achieved with a maximum adhesion of 24 N, which is nearly three times 9.5 N of the adhesion of the monolayer TiB_2 films.

References

[1] MUNRO R G. Material properties of titanium diboride [J]. J Res Natl Inst Stand Technol, 2000, 105(5): 709−720.

[2] WIEDEMANN R, OETTEL H, JERENZ M. Structure of deposited and annealed TiB_2 layers [J]. Surf Coat Technol, 1997, 97(1−3): 313−321.

[3] SADE G, PELLEG J. Co-sputtered TiB_2 as a diffusion barrier for advanced microelectronics with Cu metallization [J]. Appl Surf Sci, 1995, 91(1−4): 263−268.

[4] SHAPPIRIO J R, FINNEGAN J J. Synthesis and properties of some refractory transition metal diboride thin films [J]. Thin Solid Films, 1983, 107(1): 81−87.

[5] TAMURA M, KUBO H. Ti−B−N coatings deposited by magnetron arc evaporation [J]. Surf Coat Technol, 1992, 54−55(1): 255−260.

[6] CHEN J, BARNARD J A. Growth, structure and stress of sputtered TiB_2 thin films [J]. Mater Sci Eng A, 1995, 191(1−2): 233−238.

[7] PANICH N, SUN Y. Mechanical characterization of nanostructured TiB_2 coatings using microscratch techniques [J]. Tribol Int, 2006, 39(2): 138−145.

[8] BERGER M, CORONEL E, OLSSON E. Microstructure of d.c. magnetron sputtered TiB_2 coatings [J]. Surf Coat Technol, 2004, 185(2−3): 240−244.

[9] PANICH N, SUN Y. Effect of substrate rotation on structure, hardness and adhesion of magnetron sputtered TiB_2 coating on high speed steel [J]. Thin Solid Films, 2006, 500(1−2): 190−196.

[10] BUCHMANN M, GADOW R, TABELLION J. Experimental and numerical residual stress analysis of layer coated composites [J]. Mater Sci Eng A, 2000, 288(2): 154−159.

[11] RAMALINGAM S, ZHENG L S. Film-substrate interface stresses and their role in the tribological performance of surface coatings [J]. Tribol Int, 1995, 28(3): 145−161.

[12] BERGER M, KARLSSON L, LARSSON M, HOGMARKA S. Low stress TiB_2 coatings with improved tribological properties [J]. Thin Solid Films, 2001, 401(1−2): 179−186.

[13] PANICH N, SUN Y. Mechanical properties of TiB_2-based nanostructured coatings [J]. Surf Coat Technol, 2005, 198(1−3): 14−19.

[14] BOHWAN P, JUNG D H, KIM H, YOO K C, LEE J J, JOO J H. Adhesion properties of TiB_2 coatings on nitrided AISI H13 steel [J]. Surf Coat Technol, 2005, 200: 726−729.

[15] WANG J F, CHENG Q F, TANG Z Y. Layered nanocomposites inspired by the structure and mechanical properties of nacre [J]. Chem Soc Rev, 2012, 41(3): 1111−1129.

[16] ZHAO Y H, LIN G Q, XIAO J Q, DU H, DONG C, CAO L J. Ti/TiN multilayer thin films deposited by pulse biased arc ion plating [J]. Appl Surf Sci, 2011, 257: 2683−2688.

[17] LEE J H, KIM U W M, LEE T S, CHUNG M K, CHEONG B K, KIM S G. Mechanical and adhesion properties of Al/AlN multilayered thin films [J]. Surf Coat Technol, 2000, 133−134: 220−226.

[18] SHAN Z H, SITARAMAN S K. Elastic–plastic characterization of thin films using nanoindentation technique [J]. Thin Solid Films, 2003, 437(1−2): 176−181.

[19] MIKULA M, GRANCIC B, BURSIKOVA V, CSUBA A, DRIIK M, KAVECKY S, PLECENIK A, KUS P. Mechanical properties of superhard TiB_2 coatings prepared by DC magnetron sputtering [J]. Vacuum, 2008,82: 278−281.

[20] MORI T, FUKUDA S, TAKEMURA Y. Improvement of mechanical properties of Ti/TiN multilayer film deposited by sputtering [J]. Surf Coat Technol, 2000, 140: 122−127.

[21] RAWDANOWICZ T A, GODBOLE V, NARAYAN J, SANKAR J, SHARMA A. The hardnesses and elastic moduli of pulsed laser deposited multilayer AlN/TiN thin films [J]. Compos: Part B, 1999, 30(7): 657−665.

[22] SUNDGREN J E, HENTZELL H T G. A review of the present state of art in hard coatings grown from the vapor phase [J]. J Vac Sci Technol A, 1986, 5: 2259−2278.

[23] CHU K, LU Y H, SHEN Y G. Structural and mechanical properties of titanium and titanium diboride monolayers and Ti/TiB_2 multilayers [J]. Thin Solid Films, 2008, 516: 5313−5317.

[24] HAN X, ZHU J Q, HAN J C, TAN M L, JIA Z C, JIANG C Z. Stress, mechanical and adhesion properties of multilayer tetrahedral amorphous carbon films [J]. Appl Surf Sci, 2008, 255(2): 607−609.

[25] CAICEDO J C, AMAYA C, YATE L. Hard coating performance enhancement by using $[Ti/TiN]_n$, $[Zr/ZrN]_n$ and $[TiN/ZrN]_n$ multilayer system [J]. Mater Sci Eng B, 2010, 171: 56−60.

[26] LI G Y, HAN Z H, TIAN J W. Alternating stress field and superhardness effect in TiN/NbN superlattice films [J]. J Vac Sci Technol A, 2002, 20(3): 674−677.

[27] ANDERSON P M, LI C. Hall-Petch relations for multilayered materials [J]. Nanostruct Mater, 1995, 5(3): 349−353.

[28] QI J, LAI K H, LEE C S. Mechanical properties of a-C:H multilayer films [J]. Diamond Relat Mater, 2001, 10(9−10): 1833−1838.

Ti 层对 316L 不锈钢表面 TiB_2 薄膜结合力的影响

夏木建，丁红燕，周广宏，章 跃

淮阴工学院 江苏省介入医疗器械研究重点实验室，淮安 223001

摘　要：基于多层膜优异的力学性能，采用磁控溅射法在 316L 不锈钢基体表面沉淀$[Ti/TiB_2]_n$ (n=1,2,3)多层膜以增强 TiB_2 薄膜的膜基结合强度。研究周期数对多层膜的结构、硬度及结合力的影响。结果表明：TiB_2 单层膜表现为(001)方向的织构。随着周期数的增加，多层膜的织构方向由(001)转变为(100)；多层膜的硬度从 20 GPa 增加到 26 GPa，但略低于 TiB_2 单层膜的硬度(33 GPa)；相对于单膜的膜基结合力(9.5 N)，多层膜表现出较好膜基结合力，最大结合力可达 24 N。

关键词：多层膜；结合力；TiB_2 薄膜；磁控溅射；纳米硬度

(Edited by Chao WANG)